Table 1. Food composition of basal diet NIH-07PLD in 100 g showed A eugenol diet was produced by adding eugenol (5% w/w) to the basal pelleted diet NIH-07PLD (Oriental Yeast Co., Ltd).

Composition of NIH-07PLD	
Formula	g/100 g
White fish meal	14.00
Corn gluten meal	8.00
Corn	28.50
White flour	40.62
Brewery yeast	2.00
Cane molasses	0.75
Corn oil	2.50
Vitamin and mineral mixture	3.63

Methods

Animal diets

Eugenol was purchased from Tokyo Chemical Industry Co., Ltd. (Tokyo, Japan). A eugenol diet was produced by adding eugenol (5% w/w) to the basal pelleted diet NIH-07PLD (Oriental Yeast Co., Ltd, Tokyo, Japan). NIH-07PLD is an open-formula diet designed to contain as little phytoestrogenic substances as possible. In order to maintain a comparable levels of protein, the levels of gluten meal and white fish meal have been increased (Table 1).

Animals

Male Sprague-Dawley rats (7 weeks old; $n=6$) were housed under standard conditions and provided free access to water and NIH-07PLD pelleted diet (Oriental Yeast Co., Ltd). At 8 weeks of age, the rats were randomly divided into two groups: a control diet group (NIH-07PLD only) and a eugenol diet group (NIH-07PLD containing 5% eugenol: w/w). Body weights and food consumption were recorded every 2 days. After 4 weeks, three of the rats were sacrificed, their livers were excised and frozen immediately in liquid nitrogen before being stored at −80 °C until analysis. The section of the intestines corresponding to the jejunum was also removed and stored at −80 °C. All of the animals were treated according to the Laboratory Animal Control Guidelines at Rakuno Gakuen University, which is based on the *Guide for the Care and Use of Laboratory Animals of the U.S. National Institutes of Health*.

RNA isolation and semi-quantitative reverse-transcription polymerase chain reaction

Total RNA was isolated from livers and intestines using an RNeasy Mini kit (Qiagen, Hilden, Germany), and DNAse digestion was performed using an RNase-Free DNase kit (Qiagen NV, Hilden, Germany). Complementary DNA (cDNA) was synthesized from 1 μg of tRNA with ReverTra Ace reverse transcriptase (TOYOBO, Osaka, Japan) and oligo dT primers (Toyobo) according to the manufacturer's instructions. The coding regions of the respective cDNA species were amplified by polymerase chain reaction (PCR) with oligonucleotide primers (Supplementary Table 1).

Western blot analysis

Liver microsomal protein samples (50 μg) were subjected to gel electrophoresis on 10% sodium dodecyl sulfate-polyacrylamide gels. The polypeptide bands were transferred to a nitrocellulose membrane, and immunoreactive bands were detected using polyclonal antibodies against UGT1A6 and UGT2B1 (Ikushiro et al., 1997; Iwano et al., 1997) and followed by incubation with peroxidase-conjugated secondary antibody (Jackson ImmunoResearch Laboratories Inc., West Grove, PA).

Quantitative RT-PCR analysis

cDNA that had been diluted for the amplification of the selected genes, which were *UGT1A1*, *UGT1A6*, *UGT1A7*, *UGT2B1* and *CYP1A1*, was used for quantitative reverse-transcription polymerase chain reaction (RT-PCR) analysis. A standard curve for each gene was produced using 100-fold serial dilutions of the genes as a template (10^8–10^2 copies). The reaction was performed using a QuantiTect SYBR Green PCR kit (Qiagen) and a Light Cycler (Roche Diagnostics, Mannheim, Germany) following the manufacturer's instructions. We used same oligonucleotide primers in semi-quantitative and quantitative RT-PCR (Supplementary Table 1). The copy number of each gene expressed in the rat liver and intestine was calculated from a standard curve and normalized to that of glyceraldehyde-3-phosphate dehydrogenase (GAPDH). The quantitative values are shown as the mean ± SE for mice on the control diet ($n=3$) and mice on the eugenol diet ($n=3$).

Statistical analysis

Comparisons were made by the Student's t test, and a p value of 0.05 was taken to be significant. All values are presented as the mean ± SE.

Results

To clarify the mechanism by which eugenol influenced these genes, screening was performed by semi-quantitative RT-PCR using hepatic and intestinal total RNA. Body weights and food consumption were recorded every 2 days; these values did not differ between the two diet groups (data not shown). Hepatic and intestinal messenger RNA (mRNA) were analyzed by RT-PCR using specific primers for *CYP1A1*, *1A2*, *2B1*, *2B2*, *2C6*, *2C11*, *2D*, *2E1*, *3A1*, *3A2*, *4A1* and *UGT 1A1*, *1A2*, *1A3*, *1A6*, *1A7*, *1A8*, *1A9*, *2B1*. In the *CYP* family, eugenol treatment caused a slight reduction in the expression of *CYP1A1* in rat livers and a slight increase in the expression of *CYP2B2* in the intestines (Supplementary Figure 1). In the *UGT* family, *UGT1A1*, *UGT1A6*, *UGT1A7* and *UGT2B1* were all strongly expressed in the eugenol-treated rat livers, and these all genes were expressed at approximately the same levels in the intestines (Supplementary Figure 2). The results of the quantitative analysis using real-time PCR are shown in Figure 1. Interestingly, the level of hepatic *CYP1A 1* expression in rats fed the eugenol diet decreased to 40% that observed in the rats fed the control diet. Conversely, expression levels of hepatic *UGT1A6*, *UGT1A7* and *UGT2B1* in rats fed the eugenol diet increased by 2–3 times than observed in the control rats. While the levels of intestinal *UGT1A1*, *UGT1A6* and *UGT1A7* expression were slightly increased in both groups of rats, no statistically significant differences were observed between the control and eugenol diet groups (data not shown). These results show that eugenol specifically induces the mRNA expression of the *UGT* gene family, particularly hepatic *UGT1A6*, *UGT1A7* and *UGT2B1*, and also that it reduces the expression of hepatic *CYP1A1*. The protein levels of hepatic UGT 1A6 and UGT2B1 were also elevated in all rats administered the eugenol diet (Figure 2).

Discussion

In this study, we observed down regulation of hepatic *CYP1A1* expression and induction of hepatic *UGT1A6*, *UGT1A7* and *UGT2B1* expression by eugenol administration. Phase I enzymes,

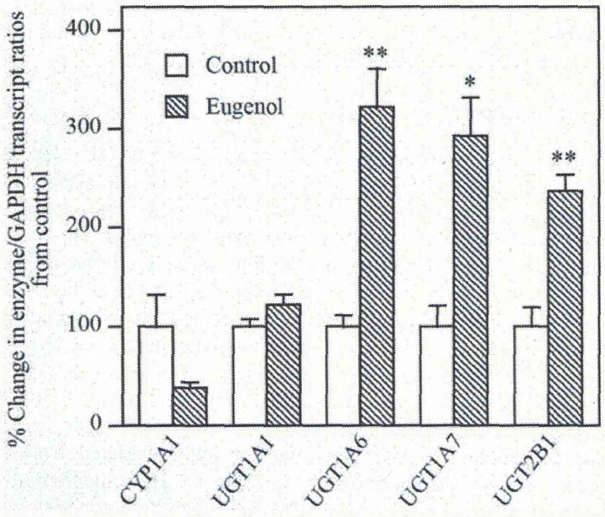

Figure 1. Quantitative analysis of gene expression by real-time RT-PCR. Quantitative analysis of mRNA expression of *Cyp1A1*, *UGT1A1*, *UGT1A6*, *UGT1A7* and *UGT2B1* in the liver of control and eugenol dietary groups were examined by real-time RT-PCR ($n = 3$, respectively). Expression of each gene in control mice was normalized to 100%. Quantitative values are shown as means ± SE. $*p < 0.05$; $**p < 0.01$ versus control.

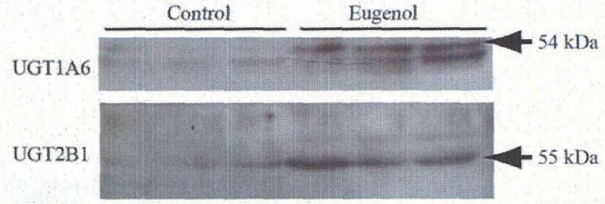

Figure 2. Effect of eugenol on levels of UGT isoforms in rat liver microsomes. Content of UGT isoforms in microsome fractions of control- and eugenol-treated liver samples were compared. The three lanes on the left contain control liver microsomes and the three lanes on the right contain eugenol-treated liver microsomes. Each lane was loaded with 50 µg of protein purified from individual animals. Arrows indicate positive bands corresponding to UGT1A6 and UGT2B1.

such as CYP1A1, are generally considered to represent an activating system for many natural and synthetic carcinogens, including polycyclic aromatic hydrocarbons (e.g. benzo[a]pyrene (BaP) and benzene) and polyhalogenated aromatic hydrocarbons (e.g. dioxin-like compounds and polychlorinated biphenyls) (Nebert & Dalton, 2006). Conversely, phase II enzymes, such as UGT (Mackenzie et al., 1997, 2003) and glutathione S-transferase (GST) (Di Pietro et al., 2010), often act to detoxify harmful natural or activated carcinogens. Consequently, inducers such as eugenol, which preferentially elevate the transcription of phase II enzymes, are expected to be beneficial because they can stimulate the detoxification of potentially carcinogenic chemicals (Kong et al., 2001; Rushmore & Kong, 2002; Xu et al., 2005). By catalyzing the transfer of glucuronic acid from UDP-glucuronic acid to predominantly hydrophobic chemicals, UGT facilitates the excretion of endogenous and xenobiotic compounds, such as bilirubin, steroids and environmental pollutants as water-soluble conjugates (Mackenzie et al., 1997, 2003). UGT 1A1 mainly catalyzes the glucuronidation of bilirubin, and absence of UGT1A1 causes Crigler–Najjar syndrome (Iyanagi et al., 1989). UGT1A6 and UGT1A7 catalyze the glucuronidation of similar substrates, such as planar phenols and BaP (Iwano et al., 1997; Mackenzie et al., 1997, 2003). UGT2B1 catalyzes the glucuronidation of a number of xenobiotics and endobiotics (steroids), such as estrogen and morphine (Mackenzie et al., 1997, 2003). We previously showed that the hepatic enzymatic activities of UGT on a variety of substrates are elevated by eugenol administration (Yokota et al., 1988). We also reported that hepatic microsomal BaP hydroxylase activity was reduced, and that the mutagenicity of BaP in the Ames test was suppressed by eugenol administration (Yokota et al., 1986). These previous observations are consistent with the present results, which showed that eugenol induced *UGT1A1*, *UGT1A6*, *UGT1A7* and *UGT2B1* expression, and reduced *CYP1A1* expression.

The expression of XME is regulated by a variety of nuclear receptors and orphan receptors, including aryl hydrocarbon receptor (AhR), constitutive androstane receptor and pregnane X receptor (Mackenzie et al., 2003; Nebert & Dalton, 2006). It has been well established that activation of AhR by exogenous compounds, such as 3-methylcholanthrene and 2,3,7,8-tetrachlorodibenzo-*p*-dioxin, promotes the nuclear transport and transcriptional activation of *CYP1A1* (Kawajiri & Fujii-Kuriyama, 2007; Pollenz, 2002). It is also been reported that the expression of hepatic CYP is reduced by lipopolysaccharide and cytokines, such as interleukin-1b and tumor necrosis factor-a, through the nuclear factor kappa B signaling pathway (Ke et al., 2001; Park et al., 2007). Indeed, further investigations need to be conducted to elucidate the detailed mechanisms underlying the suppression of CYP1A1 expression by eugenol. The induction of phase II enzymes by eugenol may also be mediated by XME receptors other than AhR, even though a specific receptor for eugenol has not yet been identified. Recent findings suggest that the *cis*-acting regulatory element and the antioxidant response element (ARE)/electrophile response element (EpRE), play important roles in the transcriptional regulation of phase II genes, such as *quinone oxidoreductase* (EC 1.6.5.2), *GST* (EC 2.5.1.18) and *UGT*, by phenolic antioxidants (Kong et al., 2001; Rushmore & Kong, 2002; Xu et al., 2005). Several ARE/EpRE-binding proteins have been identified, including the members of basic leucine zipper transcriptional factor family, nuclear factor erythroid 2-related factor 1, 2 (Nrf1, Nrf2) and small Maf proteins (Buetler et al., 1995; Hu et al., 2006). Nrf2 is the most likely transcriptional factor involved in the transcriptional activation of ARE-mediated phase II genes by a phenolic antioxidant in Nrf2−/− mice studies (Maher & Yamamoto, 2010). Indeed, elucidating which XME intermediates are involved in the eugenol signaling pathway should be investigated in the future. Eugenol has been demonstrated to inhibit prostaglandin biosynthesis and to block COX-2 activity (Kim et al., 2003) and has been shown to be a potent inhibitor of melanoma cell proliferation through the suppression of the E2F transcriptor factor family (Ghosh et al., 2005). These studies suggest that dietary eugenol is beneficial and that it has anti-inflammatory and anti-cancer properties. In long-term carcinogenicity experiments conducted by various groups in CD-1 mice and F344 rats, eugenol was not associated with tumor formation. In addition, the National Toxicology Program concluded that eugenol was not carcinogenic to rats and that there was no evidence that unequivocally proved the carcinogenic nature of eugenol in mice (Report, 1983).

Conclusions

This study demonstrates that the natural compound eugenol improves the xenobiotic-metabolizing systems that suppress and induce the expression of *CYP1A1* and *UGT*, respectively. These suggesting that eugenol could potentially be used as an anticancer drug through maintaining the homeostasis of xenobiotic metabolism.

Declaration of interest

H. Iwano participated in study design and organized all experiments. W. U. and M. N. treated animal and performed quantitative RT-PCR analysis. S. I. helped to draft the manuscript. H. Inoue helped statistical analysis. All authors have read and approved the manuscript.

This work was partially supported by Grants-in-Aid to cooperative Research from Rakuno Gakuen University. Rakuno Gakuen University Dairy Science Institute, 2006 and a Feasibility Study among Fundamental Studies under the framework of EXTEND 2010 (Extended Tasks on Endocrine Disruption 2010) funded by the Ministry of the Environment, Japan.

Reference

Aggarwal BB, Kunnumakkara AB, Harikumar KB, Tharakan ST, Sung B, Anand P. 2008. Potential of spice-derived phytochemicals for cancer prevention. Planta Medica 74:1560–1569.

Aggarwal BB, Shishodia S. 2006. Molecular targets of dietary agents for prevention and therapy of cancer. Biochem Pharmacol 71:1397–1421.

Barry H, Cole SPC, Kuchler K, Higgins CF. 2003. ABC proteins: from bacteria to man. Academic Press.

Buetler TM, Gallagher EP, Wang C, Stahl DL, Hayes JD, Eaton DL. 1995. Induction of phase I and phase II drug-metabolizing enzyme mRNA, protein, and activity by BHA, ethoxyquin, and oltipraz. Toxicol Appl Pharmacol 135:45–57.

Di Pietro G, Magno LA, Rios-Santos F. 2010. Glutathione S-transferases: an overview in cancer research. Expert Opin Drug Metab Toxicol 6: 153–170.

Ghosh R, Nadiminty N, Fitzpatrick JE, Alworth WL, Slaga TJ, Kumar AP. 2005. Eugenol causes melanoma growth suppression through inhibition of E2F1 transcriptional activity. J Biol Chem 280: 5812–5819.

Hediger MA, Romero MF, Peng JB, Rolfs A, Takanaga H, Bruford EA. 2004. The ABCs of solute carriers: physiological, pathological and therapeutic implications of human membrane transport proteins. Pflugers Arch 447:465–468.

Hu R, Shen G, Yerramilli UR, Lin W, Xu C, Nair S, Kong AN. 2006. In vivo pharmacokinetics, activation of MAPK signaling and induction of phase II/III drug metabolizing enzymes/transporters by cancer chemopreventive compound BHA in the mice. Arch Pharm Res 29: 911–920.

Ikushiro S, Emi Y, Iyanagi T. 1997. Protein–protein interactions between UDP-glucuronosyltransferase isozymes in rat hepatic microsomes. Biochemistry 36:7154–7161.

Iwano H, Yokota H, Ohgiya S, Yotumoto N, Yuasa A. 1997. A critical amino acid residue, asp446, in UDP-glucuronosyltransferase. Biochem J 325:587–591.

Iyanagi T, Watanabe T, Uchiyama Y. 1989. The 3-methylcholanthrene-inducible UDP-glucuronosyltransferase deficiency in the hyperbilirubinemic rat (Gunn rat) is caused by a-1 frameshift mutation. J Biol Chem 264:21302–21307.

Kamatou GP, Vermaak I, Viljoen AM. 2012. Eugenol – from the remote Maluku islands to the international market place: a review of a remarkable and versatile molecule. Molecules 17:6953–6981.

Kawajiri K, Fujii-Kuriyama Y. 2007. Cytochrome P450 gene regulation and physiological functions mediated by the aryl hydrocarbon receptor. Arch Biochem Biophys 464:207–212.

Ke S, Rabson AB, Germino JF, Gallo MA, Tian Y. 2001. Mechanism of suppression of cytochrome P-450 1A1 expression by tumor necrosis factor-alpha and lipopolysaccharide. J Biol Chem 276:39638–39644.

Kim SS, Oh OJ, Min HY, Park EJ, Kim Y, Park HJ, Nam Han Y, Lee SK. 2003. Eugenol suppresses cyclooxygenase-2 expression in lipopolysaccharide-stimulated mouse macrophage RAW264.7 cells. Life Sci 73:337–348.

Kong AN, Owuor E, Yu R, Hebbar V, Chen C, Hu R, Mandlekar S. 2001. Induction of xenobiotic enzymes by the MAP kinase pathway and the antioxidant or electrophile response element (ARE/EpRE). Drug Metab Rev 33:255–271.

Mackenzie PI, Gregory PA, Gardner-Stephen DA, Lewinsky RH, Jorgensen BR, Nishiyama T, Xie W, Radominska-Pandya A. 2003. Regulation of UDP glucuronosyltransferase genes. Curr Drug Metab 4: 249–257.

Mackenzie PI, Owens IS, Burchell B, Bock KW, Bairoch A, Belanger A, Fournel-Gigleux S, et al. 1997. The UDP glycosyltransferase gene superfamily: recommended nomenclature update based on evolutionary divergence. Pharmacogenetics 7:255–269.

Maher J, Yamamoto M. 2010. The rise of antioxidant signaling – the evolution and hormetic actions of Nrf2. Toxicol Appl Pharmacol 244: 4–15.

Manikandan P, Murugan RS, Priyadarsini RV, Vinothini G, Nagini S. 2010. Eugenol induces apoptosis and inhibits invasion and angiogenesis in a rat model of gastric carcinogenesis induced by MNNG. Life Sci 86:936–941.

Nebert DW, Dalton TP. 2006. The role of cytochrome P450 enzymes in endogenous signalling pathways and environmental carcinogenesis. Nat Rev Cancer 6:947–960.

Nebert DW, Gonzalez FJ. 1987. P450 genes: structure, evolution, and regulation. Ann Rev Biochem 56:945–993.

Nelson DR, Kamataki T, Waxman DJ, Guengerich FP, Estabrook RW, Feyereisen R, Gonzalez FJ, et al. 1993. The P450 superfamily: update on new sequences, gene mapping, accession numbers, early trivial names of enzymes, and nomenclature. DNA Cell Biol 12:1–51.

Park KR, Lee JH, Choi C, Liu KH, Seog DH, Kim YH, Kim DE, et al. 2007. Suppression of interleukin-2 gene expression by isoeugenol is mediated through down-regulation of NF-AT and NF-kappaB. Int Immunopharmacol 7:1251–1258.

Pisano M, Pagnan G, Loi M, Mura ME, Tilocca MG, Palmieri G, Fabbri D, et al. 2007. Antiproliferative and pro-apoptotic activity of eugenol-related biphenyls on malignant melanoma cells. Mol Cancer 6:8–19.

Pollenz RS. 2002. The mechanism of AH receptor protein down-regulation (degradation) and its impact on AH receptor-mediated gene regulation. Chem Biol Interact 141:41–61.

Rushmore TH, Kong AN. 2002. Pharmacogenomics, regulation and signaling pathways of phase I and II drug metabolizing enzymes. Curr Drug Metab 3:481–490.

Xu C, Li CY, Kong AN. 2005. Induction of phase I, II and III drug metabolism/transport by xenobiotics. Arch Pharm Res 28:249–268.

Yokota H, Hashimoto H, Motoya M, Yuasa A. 1988. Enhancement of UDP-glucuronyltransferase, UDP-glucose dehydrogenase, and glutathione S-transferase activities in rat liver by dietary administration of eugenol. Biochem Pharmacol 37:799–802.

Yokota H, Hoshino J, Yuasa A. 1986. Suppressed mutagenicity of benzo[a]pyrene by the liver S9 fraction and microsomes from eugenol-treated rats. Mutat Res 172:231–236.

Yoo CB, Han KT, Cho KS, Ha J, Park HJ, Nam JH, Kil UH, Lee KT. 2005. Eugenol isolated from the essential oil of *Eugenia caryophyllata* induces a reactive oxygen species-mediated apoptosis in HL-60 human promyelocytic leukemia cells. Cancer Lett 225:41–52.

Report. 1983. Carcinogenesis studies of eugenol in F344/N rats and B6C3F1 mice. National Toxicology Program Technical Report Series, No. 223.

Supplementary material available online

Supplementary Table 1 and Figures 1 and 2.

OPEN ACCESS Freely available online

PLOS | ONE

Latrunculin A Treatment Prevents Abnormal Chromosome Segregation for Successful Development of Cloned Embryos

Yukari Terashita[1,2*], Kazuo Yamagata[1,3], Mikiko Tokoro[1,4], Fumiaki Itoi[1,4], Sayaka Wakayama[1,7], Chong Li[1,5], Eimei Sato[2,6], Kentaro Tanemura[2], Teruhiko Wakayama[1,7*]

1 Laboratory for Genomic Reprogramming, Center for Developmental Biology, RIKEN, Kobe, Japan, **2** Laboratory of Animal Reproduction, Graduate School of Agricultural Science, Tohoku University, Sendai, Japan, **3** Center for genetic analysis of biological responses, Research Institute for Microbial Diseases, Osaka University, Suita, Japan, **4** Asada Institute for Reproductive Medicine, Asada Ladies Clinic, Kasugai, Japan, **5** School of Medicine, Tongji University, Shanghai, China, **6** Managing director, National Livestock Breeding Center, Nishishirakawa-gun, Japan, **7** Department of Biotechnology, Faculty of Life and Environmental Science, University of Yamanashi, Kofu, Japan

Abstract

Somatic cell nuclear transfer to an enucleated oocyte is used for reprogramming somatic cells with the aim of achieving totipotency, but most cloned embryos die in the uterus after transfer. While modifying epigenetic states of cloned embryos can improve their development, the production rate of cloned embryos can also be enhanced by changing other factors. It has already been shown that abnormal chromosome segregation (ACS) is a major cause of the developmental failure of cloned embryos and that Latrunculin A (LatA), an actin polymerization inhibitor, improves F-actin formation and birth rate of cloned embryos. Since F-actin is important for chromosome congression in embryos, here we examined the relation between ACS and F-actin in cloned embryos. Using LatA treatment, the occurrence of ACS decreased significantly whereas cloned embryo-specific epigenetic abnormalities such as dimethylation of histone H3 at lysine 9 (H3K9me2) could not be corrected. In contrast, when H3K9me2 was normalized using the G9a histone methyltransferase inhibitor BIX-01294, the *Magea2* gene—essential for normal development but never before expressed in cloned embryos—was expressed. However, this did not increase the cloning success rate. Thus, non-epigenetic factors also play an important role in determining the efficiency of mouse cloning.

Citation: Terashita Y, Yamagata K, Tokoro M, Itoi F, Wakayama S, et al. (2013) Latrunculin A Treatment Prevents Abnormal Chromosome Segregation for Successful Development of Cloned Embryos. PLoS ONE 8(10): e78380. doi:10.1371/journal.pone.0078380

Editor: Zhongjun Zhou, The University of Hong Kong, Hong Kong

Received July 24, 2013; **Accepted** September 20, 2013; **Published** October 24, 2013

Funding: Financial support for this research was provided by Research Fellow of the Japan Society for the Promotion of Science to YT and Grant-in-Aid for Scientific Research on Priority Areas (20062015) and Scientific Research (A) (23248048) to TW. The funders had no role in study design, data collection and analysis, decision to publish, or preparation of the manuscript.

Competing interests: *The authors have declared that no competing interests exist.*

* E-mail: yterashita@cdb.riken.jp(YT); twakayama@yamanashi.ac.jp (TW)

Introduction

The oocyte's reprogramming ability to reset the genomic specialization of a somatic nucleus is the most efficient method used so far for cloning [1,2] and can give rise to full-term cloned animals [3,4]. Since cloned mice were first produced in 1998 [4], there have been many attempts at improving the birth rate [5], such as modifying the methodology [4,6], controlling the DNA acetylation status [7] and changing the timing of oocyte enucleation [8]. However, many disparities remained between normally fertilized embryos and cloned embryos and the birth rates of cloned embryos are still very low. The main cause of these problems is regarded as the incomplete reprogramming of the somatic epigenome and there have many studies aimed at improving the epigenetic status of cloned embryos [6,7,9-11]. However, some clone-specific epigenetic abnormalities, such as dimethylation of histone H3 at lysine 9 (H3K9me2), have never been corrected to the same level as in normally fertilized embryos by any treatment [12,13], whereas treatment with trichostatin A (TSA) improved the success rate of cloned mice by correcting other epigenetic abnormalities.

Here, we tried to improve the birth rate of cloned mice produced by somatic cell nuclear transfer (SCNT) in terms of alleviating both genetic and epigenetic problems in cloned embryos. For the epigenetic approach, we focused on H3K9me2, which serves as a binding region for heterochromatin protein 1 (HP1) [14,15]. HP1 localizes to

Journal of Reproduction and Development, Vol. 59, No 4, 2013

—Technology Report—

Selection of *In Vitro*-Matured Porcine Oocytes Based on Localization Patterns of Lipid Droplets to Evaluate Developmental Competence

Kou HIRAGA[1)], Yumi HOSHINO[1)], Kentaro TANEMURA[1)] and Eimei SATO[1)]

[1)]*Laboratory of Animal Reproduction, Graduate School of Agricultural Science, Tohoku University, Sendai 981-8555, Japan*

Abstract. Localization patterns of lipid droplets in the cytoplasm of porcine oocytes were evaluated as a novel marker for *in vitro* maturation (IVM) of oocytes with high developmental competence. Porcine oocytes were cultured in TCM-199, which is a complete synthetic medium, for 44 h at 38.5 C. Localization patterns were divided into 2 classes: lipid droplets localized uniformly in the whole cytoplasm (class I) and those that were centrally located (class II). After IVM in TCM-199, 60% of matured oocytes exhibited the class II pattern. To investigate the relation between the distribution of lipid droplets and the developmental rate of the oocyte, the developmental rates of class I and class II oocytes were compared after *in vitro* fertilization (IVF). Class II oocytes showed a significantly higher rate of blastocyst development than class I oocytes. These results suggest that porcine oocytes with high developmental competence can be selected based on the localization patterns of lipid droplets.
Key words: Lipid droplet, Novel marker, Porcine oocyte

(**J. Reprod. Dev. 59:** 405–408, 2013)

Porcine embryos from *in vitro* maturation (IVM) and *in vitro* fertilization (IVF) develop into blastocysts under *in vitro* conditions [1–3]; however, the developmental rates are very low compared with those of oocytes matured and fertilized *in vivo* [1, 3–6]. One factor contributing to this low developmental rate has been thought to be incomplete cytoplasmic maturation of the oocytes that mature *in vitro* [7]. Therefore, considerable improvement has been made to the IVM medium in which porcine oocytes are matured [7, 8]. A frequently used standard medium for IVM of porcine oocytes is North Carolina State University (NCSU)-23 [5] with porcine follicular fluid (pFF) supplementation [9–11]; however, follicular fluid contains numerous undefined factors and can be contaminated with viral pathogens [12–15]. Application of a fully defined IVM system eliminating follicular fluid from the medium could decrease the risk of viral contamination during *in vitro* production (IVP) of embryos. Tissue culture medium (TCM)-199, a complete synthetic medium for oocyte maturation, has been used in many laboratories [2, 16–18]. Blastocyst development [1, 2, 16, 17] and the birth of piglets [16] from oocytes matured in TCM-199 have been reported, although the efficiency has remained low.

To make the IVP system more stable for porcine oocytes using a complete synthetic medium, blastocyst production rate and quality had to be improved. Selection of IVM oocytes with high grades of cytoplasmic maturation for IVF would make further steps more easy by removing low-potential oocytes, saving time and materials and thus costs. Also, the quality of blastocysts, and developmental rate may improve. To do so, a simple, quick, and highly precise method for the evaluation of cytoplasmic maturity is needed. Using stereomicroscopic evaluation, immature oocytes appeared uniform in term of lipid droplet distribution in the cytoplasm (Fig. 1). We observed and classified the localization patterns of lipid droplets in matured oocytes after IVM in TCM-199 with stereomicroscope observation. In "class I" oocyte the lipid droplets were uniformly distributed throughout the entire cytoplasm, whereas in "class II" oocytes, the lipid droplets were centrally located in the cytoplasm (Fig. 2). As a result, significantly ($P<0.01$) more class II oocytes (% ± SEM = 60.9 ± 1.6) were observed after IVM than class I oocytes (27.3 ± 2.6). The remaining 11.8% of oocytes were degraded. The accuracy of classification of lipid droplet distribution by stereomicroscopy was verified by fluorescent lipid-specific staining (Fig. 2). To investigate the relationship between the distribution of lipid droplets and developmental rate, we compared developmental ability of class I and class II oocytes after IVF (Table 1). The blastocyst developmental rate of class II oocytes was significantly ($P<0.05$) higher than that of class I oocytes. However, cell number of the blastocyst was no different. That is, after IVM in TCM-199, the oocytes in which lipid droplets were centrally located had a higher developmental rate. The results suggest that the localization pattern of lipid droplets in porcine IVM oocytes can be an important indicator for selecting oocytes with high developmental competence.

The change in the localization of the cortical granules or mitochondria in IVM had previously been reported as a morphological marker of cytoplasmic maturation [19–21]. However, for such investigations, oocytes have to be fixed and dyed during evaluation, and they then cannot be used for *in vitro* fertilization and *in vitro* culture after IVM. The localization pattern of lipid droplets after IVM that became clear in our study is a morphological character that is observation without dye, enabling simple and quick evaluation of live oocytes. Evaluation of lipid droplet localization pattern in porcine IVM oocytes may also be a useful tool for clarifying the relationship between cytoplasmic maturation and developmental competence.

Sturmey and Leese reported that the level of triglycerides, which are main ingredients in lipid droplets in immature porcine oocytes decreased during IVM [22]. In addition, Somfai *et al.* reported that the

Received: August 29, 2012
Accepted: March 10, 2013
Published online in J-STAGE: April 18, 2013

Correspondence: K Hiraga (e-mail: b2ad1209@s.tohoku.ac.jp)

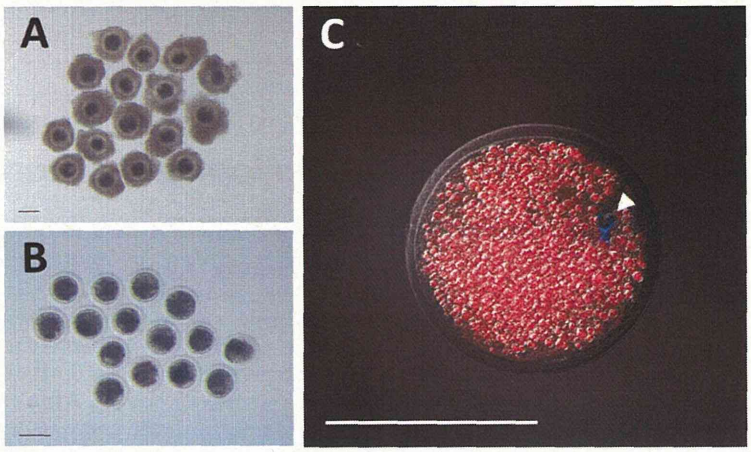

Fig. 1. Status of lipid droplets in porcine germinal vesicle (GV) oocytes. A: Selected COCs for IVM. B: Denuded GV oocyte. C: Immunostaining of lipid droplets. Intracellular lipids and DNA were stained by Nile red (red) and Hoechst 33342 (blue; arrowhead), respectively. Scale bar = 100 μm.

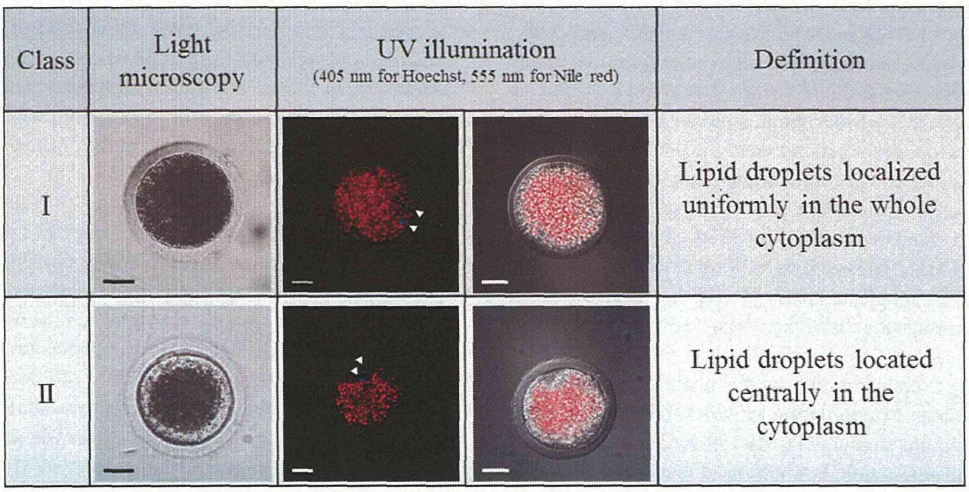

Fig. 2. Classification of localization patterns of lipid droplets in porcine oocytes after IVM. Intracellular lipids and DNA were stained by Nile red (red) and Hoechst 33342 (blue; arrowheads), respectively. Scale bar = 30 μm.

Table 1. Developmental competence of matured porcine oocytes with different localization patterns of lipid droplets

Lipid droplet distribution	No. of oocytes	Cleavage at Day 2 (%)	Blastocyst at Day 7 (%)	Cell number/ blastocyst
Class I	77	64 (85.3 ± 3.4)	3 (3.3 ± 2.1)[b]	48.7 ± 14.3
Class II	138	110 (80.6 ± 3.8)	23 (16.4 ± 3.6)[a]	50.6 ± 4.9

%: Mean ± SD. Day means day after fertilization. Different superscripts within columns indicate significant differences ($P<0.05$; 6 replicates).

addition of L-carnitine to the maturation medium, which enhances lipid metabolism, decreased intracellular lipids in porcine oocytes and improved maturation rate and division capability [23]. In accordance with these reports, our research suggests that lipid metabolism in porcine oocytes had an effect on cytoplasmic maturation in IVM and subsequent embryonic growth.

Methods

In vitro maturation

Ovaries were collected from prepubertal gilts at a local slaughterhouse and transported to the laboratory in a container within 2 h of

extraction. The follicular fluid and porcine oocytes were aspirated from antral follicles (diameter: 3–6 mm) by using a 10-ml syringe attached to an 18-gauge needle. Compact cumulus-oocyte complexes (COCs) with uniformly granulated cytoplasm were selected in PBS supplemented with 0.1% polyvinyl alcohol (PVA; Sigma, St. Louis, USA). After washing in 0.1% PBS-PVA, the COCs were cultured in TCM-199 supplemented with 2.2 mg/ml sodium bicarbonate (Sigma), 570 μM cysteamine (Sigma), 10 ng/ml EGF (Sigma), 100 mIU/ml FSH (Sigma), 100 IU/ml penicillin G (Gibco, Grand Island, USA), and 100 mg/ml streptomycin (Gibco). Groups of 25 oocytes were cultured in 250 μl of medium microdroplets for 44 h in an atmosphere containing 5% CO_2 at 38.5 C. Each droplet of medium was overlaid with liquid paraffin (Nacalai Tesque, Kyoto, Japan) in a 35-mm dish (Sumitomo Bakelite, Tokyo, Japan). At the end of culture, cumulus cells were removed from oocytes by glass micropipette after treatment with 0.1% hyaluronidase (Sigma) at room temperature.

Selection of lipid droplet localization patterns

After IVM, matured oocytes exposing the first polar body were selected under a stereomicroscope (Olympus, SZ-40, Tokyo, Japan) and used for subsequent experiments. Matured oocytes were observed with a stereomicroscope and classified according to the localization patterns of the lipid droplets. The standard classification of lipid droplet distribution was performed by using the public domain ImageJ program (developed at the U.S. National Institutes of Health and available on the Internet at http://rsb.info.nih.gov/ij). Matured oocytes were photographed using an inverted microscope (Olympus, IX70) and photography software (Olympus, DP2-BSW), and the pictures were transformed into 8-bit grayscale images. The area of the oocyte measured in the number of pixels, and the percentage of the total oocyte area occupied by lipid droplets was computed. An area showing a pixel intensity of 50 or less was assumed to be occupied by lipid droplets. In "class I" oocytes, the lipid droplets were uniformly distributed throughout the entire cytoplasm, whereas in "class II" oocytes, the lipid droplets were centrally located and covered less than 70% of the cytoplasm.

Evaluation of lipid droplets and chromosomes by confocal laser scanning microscopy

Oocytes were stained by the method of X-W Fu *et al.* with some modifications [24]. Denuded oocytes were fixed with 4% paraformaldehyde (Sigma) in phosphate-buffered saline (PBS) containing 0.1% polyvinyl alcohol (PBS-PVA) for at least 90 min at room temperature. The fixed oocytes were then rinsed three times in PBS-PVA, for 5 min each, and treated overnight with 10 μg/ml Nile red solution (Invitrogen, Grand Island, USA) dissolved in PBS-PVA at room temperature. The Nile red stock solution (1 mg/ml) was prepared by dilution in dimethyl sulfoxide (DMSO; Sigma) and stored at room temperature in the dark. Final concentrations were obtained by diluting the stock with saline solution. The following morning, they were briefly washed in PBS-PVA and stained with 5 μg/ml Hoechst 33342 (Sigma) in PBS-PVA for 20 min at room temperature. After being washed two additional times in PBS (5 min each), oocytes were mounted on nonfluorescent slides and observed under a confocal laser-scanning microscope (Zeiss LSM700, Oberkochen, Germany). Each treatment was repeated at least three times.

In vitro fertilization and culture

The methods for IVF and IVC were based on those described by Kikuchi *et al.* (2002) [11]. Epididymides from a Landrace boar were obtained, and epididymal spermatozoa were collected and frozen. Spermatozoa were thawed and preincubated for 30 min at 38.5 C in TCM-199 adjusted to pH 7.8. Fertilization medium (Pig-FM) for porcine oocytes consisting of 90 mM NaCl, 12 mM KCl, 25 mM $NaHCO_3$, 0.5 mM NaH_2PO_4, 0.5 mM $MgSO_4$, 10 mM sodium lactate (Kanto Chemical, Tokyo, Japan), and 10 mM HEPES was modified further by adding 8 mM CaCl2, 2 mM sodium pyruvate (Sigma), 2 mM caffeine, and 5 mg/ml BSA (Fraction V; Sigma). A portion (10 μl) of the preincubated spermatozoa was introduced into 90 μl of fertilization medium containing approximately 10 denuded oocytes. The final sperm concentration was adjusted to 1×10^5/ml. *In vitro* fertilization was carried out at 38.5 C under 5% CO_2. After IVF for 3 h, all putative zygotes were freed from the attached spermatozoa and transferred into IVC medium. The day of insemination was defined as day 0. The basic IVC medium was NCSU-37 containing 4 mg/ml BSA (Sigma) and 50 mM β-mercaptoethanol. Two types of IVC medium were prepared: 1) basic supplemented with 0.17 mM sodium pyruvate and 2.73 mM sodium lactate (IVC-PyrLac) and 2) basic with 5.55 mM D-glucose (IVC-Glu; Wako, Osaka, Japan), as originally reported [5]. Groups of 20 oocytes were cultured in 500 μl of IVC-PyrLac for 48 h, and then incubated in the IVC-Glu for an additional 120 h in an atmosphere containing 5% CO_2 at 38.5 C. Each droplet of medium was overlaid with liquid paraffin (Nacalai Tesque) in 4-well dishes (Nunc). These experiments were repeated at least five times.

Evaluation of embryo development

To examine their ability to develop into the blastocyst stage *in vitro*, all embryos and oocytes were cultured for 7 days, fixed and stained with 5 μg/ml Hoechst 33342 in PBS supplemented with 0.1% PVA; embryos were mounted on nonfluorescent slides and observed under a confocal laser-scanning microscope (Zeiss LSM700). An embryo with a clear blastocoel was defined as a blastocyst for the purposes of this study. The rate of blastocyst formation was evaluated, and the total number of cells in each blastocyst was evaluated as an indicator of embryo quality.

Statistical analysis

Statistical analyses were carried out using analysis of variance (ANOVA) and Fisher's protected least significant difference test using StatView. Differences of $P<0.05$ were considered significant.

Acknowledgments

We thank the staff of the Meat Inspection Office, Sendai City, Japan, for supplying the porcine ovaries. This work was supported by a Japan Society for the Promotion of Science grant to ES (No. 21248032).

References

1. **Nagashima H, Nagai T, Yamakawa H.** *In vitro* development of *in vivo* and *in vitro* fertilized pig zygotes. *J Reprod Dev* 1993; **2**: 163–168.
2. **Funahashi H, Cantley TC, Stumpf TT, Terlouw SL, Day BN.** *In vitro* development of *in vitro*-matured porcine oocytes following chemical activation or *in vitro* fertilization. *Biol Reprod* 1994; **50**: 1072–1077. [Medline]
3. **Rath D, Niemann H, Torres CR.** *In vitro* development to blastocysts of early porcine embryos produced *in vivo* or *in vitro*. *Theriogenology* 1995; **43**: 913–926. [Medline]
4. **Beckmann LS, Day BN.** Effects of media NaCl concentration and osmolarity on the culture of early-stage porcine embryos and the viability of embryos cultured in a selected superior medium. *Theriogenology* 1993; **39**: 611–622. [Medline]
5. **Petters RM, Wells KD.** Culture of pig embryos. *J Reprod Fertil Suppl* 1993; **48**: 61–73. [Medline]
6. **Dobrinsky JR, Johnson LA, Rath D.** Development of a culture medium (BECM-3) for porcine embryos: effects of bovine serum albumin and fetal bovine serum on embryo development. *Biol Reprod* 1996; **55**: 1069–1074. [Medline]
7. **Niwa K.** Effectiveness of *in vitro* maturation and *in vitro* fertilization techniques in pigs. *J Reprod Fertil Suppl* 1993; **48**: 49–59. [Medline]
8. **Nagai T.** *In vitro* maturation and fertilization of pig oocyte. *Anim Reprod Sci* 1996; **42**: 153–163.
9. **Funahashi H, Kim NH, Stumpf TT, Cantly TC, Day BN.** Presence of organic osmolytes in maturation medium enhances cytoplasmic maturation porcine oocyte. *Biol Reprod* 1996; **54**: 1412–1419. [Medline]
10. **Funahashi H, Cantley TC, Day BN.** Synchronization of meiosis in porcine oocytes by exposure to dibutyryl cyclic adenosine monophosphate improves developmental competence following *in vitro* fertilization. *Biol Reprod* 1997; **57**: 49–53. [Medline]
11. **Kikuchi K, Onishi A, Kashiwazaki N, Iwamoto M, Noguchi J, Kaneko H, Akita T, Nagai T.** Successful piglet production after transfer of blastocysts produced by a modified *in vitro* system. *Biol Reprod* 2002; **66**: 1033–1041. [Medline]
12. **Sur JH, Doster AR, Galeota JA, Osorio FA.** Evidence for the localization of porcine reproductive and respiratory syndrome virus (PRRSV) antigen and RNA in ovarian follicles in gilts. *Vet Pathol* 2001; **38**: 58–66. [Medline]
13. **Galik PK, Givens MD, Stringfellow DA, Crichton EG, Bishop MD, Eilertsen KJ.** Bovine viral diarrhea virus (BVDV) and anti-BVDV antibodies in pooled samples of follicular fluid. *Theriogenology* 2002; **57**: 1219–1227. [Medline]
14. **Devaux A, Soula V, Sifer C, Branger M, Naouri M, Porcher R, Poncelet C, Neuraz A, Alvarez S, Benifla JL, Madelenat P, Brun-Vazinet F, Feldmann G.** Hepatitis C virus detection in follicular fluid and culture media from HCV+ women, and viral risk during IVF procedures. *Hum Reprod* 2003; **18**: 2342–2349. [Medline]
15. **Pogranichniy R, Lee K, Machaty Z.** Detection of porcine parvovirus in the follicular fluid of abattoir pigs. *J Swine Health Prod* 2008; **16**: 244–246.
16. **Mattioli M, Bacci ML, Galeati G, Seren E.** Developmental competence of pig oocytes matured and fertilized *in vitro*. *Theriogenology* 1989; **31**: 1201–1207. [Medline]
17. **Yoshida M, Ishizaki Y, Kawagishi H.** Blastocyst formation by pig embryos resulting from *in-vitro* fertilization of oocytes matured *in vitro*. *J Reprod Fertil* 1990; **88**: 1–8. [Medline]
18. **Wang WH, Niwa K, Okuda K.** *In-vitro* penetration of pig oocytes matured in culture by frozen-thawed ejaculated spermatozoa. *J Reprod Fertil* 1991; **93**: 491–496. [Medline]
19. **Wang WH, Sun QY, Hosoe M, Shioya Y, Day BN.** Quantified analysis of cortical granule distribution and exocytosis of porcine oocytes during meiotic maturation and activation. *Biol Reprod* 1997; **56**: 1376–1382. [Medline]
20. **Sun QY, Wu GM, Lai L, Park KW, Cabot R, Cheong HT, Day BN, Prather RS, Schatten H.** Translocation of active mitochondria during pig oocyte maturation, fertilization and early embryo development *in vitro*. *Reproduction* 2001; **122**: 155–163. [Medline]
21. **Sha W, Xu BZ, Li M, Liu D, Feng HL, Sun QY.** Effect of gonadotropins on oocyte maturation *in vitro*: an animal model. *Fertil Steril* 2010; **93**: 1650–1661. [Medline]
22. **Sturmey RG, Leese HJ.** Energy metabolism in pig oocytes and early embryos. *Reproduction* 2003; **126**: 197–204. [Medline]
23. **Somfai T, Kaneda M, Akagi S, Watanabe S, Haraguchi S, Mizutani E, Dang-Nguyen TQ, Geshi M, Kikuchi K, Nagai T.** Enhancement of lipid metabolism with L-carnitine during *in vitro* maturation improves nuclear maturation and cleavage ability of follicular porcine oocytes. *Reprod Fertil Dev* 2011; **23**: 912–920. [Medline]
24. **Fu XW, Wu GQ, Li JJ, Hou YP, Zhou GB, Suo L, Wang YP, Zhu SE.** Positive effects of Forskolin (stimulator of lipolysis) treatment on cryosurvival of *in vitro* matured porcine oocytes. *Theriogenology* 2011; **75**: 268–275. [Medline]

heterochromatin domains [16] and is involved in downregulation of the *Magea* and *Xlr* family genes [10]. These genes have never been expressed in any cloned embryos even when genetically manipulated donor cells were used [6,10]. For the non-epigenetic approach, we focused on abnormal chromosome segregation (ACS). Although it is not clear whether ACS in cloned embryos is biologically or technically problem [17] and Balbach et al. reported that the karyotypes and chromosome segregation in cloned mouse embryos are not as bad either [18,19], at least some cloned embryos showed ACS and we recently reported that the birth rate of cloned mice could be improved by modifying the protocol rather than via epigenetic alteration [20]. Generally, reconstructed oocytes should be treated with actin polymerization inhibitors such as cytochalasin B (CB) or D during activation to keep all chromosomes inside the ooplasm, otherwise pseudo-second polar bodies can be extruded and some chromosomes derived from the donor nucleus will be lost [21]. Nevertheless, we found that F-actin localization in CB-treated cloned embryos was different from that seen in normally fertilized embryos. When we used latrunculin A (LatA)—a G-actin polymerization inhibitor —instead of CB, all chromosomes were kept inside the ooplasm without adverse effects on F-actin and the birth rate of cloned mice was increased [20]. Actin is an abundant protein present in all eukaryotic cells, and actin polymerization and depolymerization play fundamental roles in biological processes such as cell migration, determining cell shape, vesicle trafficking and regulating transcription [1,2,22,23]. It is also known that the F-actin meshwork that forms in the nuclear space is essential for preventing chromosome loss and aneuploidy in the embryo [24]. Such aneuploidy is one of the main causes of death in cloned embryos [25].

In the present study, we used live cell imaging to examine how LatA treatment affected the full-term development of cloned embryos not only in terms of epigenetic factors such as histone modifications and gene expression, but also for non-epigenetic factors such as chromosome segregation in early embryogenesis. In addition, we tried to correct H3K9me2 in cloned embryos using BIX-01294 (BIX) [26]. This is a specific inhibitor of the G9a histone methyltransferase responsible for dimethylation of H3K9 at transcriptionally silent regions [27,28]. However, this attempted correction of H3K9me2 did not improve the successful full-term development rate of cloned embryos.

Materials and Methods

Animals

B6D2F1 (C57BL/6 × DBA/2) strain female mice, aged 8–10 weeks, were used to produce oocytes. The surrogate pseudopregnant female mice used as embryo transfer recipients (see below) were ICR strain mice mated with vasectomized male mice of the same strain. B6D2F1 and ICR mice were purchased from Shizuoka Laboratory Animal Center (Hamamatsu, Japan). All animal experiments conformed to the Guide for the Care and Use of Laboratory Animals and were approved by the Institutional Committee of Laboratory Animal Experimentation of the RIKEN Center for Developmental Biology.

Collection of oocytes

Mature oocytes were collected from the oviducts of 8–10-week-old female mice that had been induced to superovulate with 5 IU pregnant mare serum gonadotropin (Teikokuzoki, Tokyo, Japan) followed by 5 IU human chorionic gonadotropin (hCG, Teikokuzoki) 48 h later. Cumulus-oocyte complexes (COCs) were collected from the oviducts approximately 16 h after hCG injection. After collection, COCs were placed in HEPES-buffered CZB medium (H-CZB) [29] and treated with 0.1% bovine testicular hyaluronidase (Sigma-Aldrich, St Louis, MO, USA). After several minutes, the cumulus-free oocytes were washed twice and then cultured in a droplet of potassium simplex optimized medium (KSOM) (Millipore [U.K.] Ltd., Watford, UK) at 37 °C under 5% CO_2 in air until used.

ICSI

Spermatozoa were collected from the cauda epididymidis of a mature B6D2F1 male mouse and incubated in H-CZB medium for more than 30 min at room temperature. ICSI was performed as described [30]. Briefly, the sperm head was separated from the tail by applying several piezo pulses to the neck region and the head was then injected into an oocyte. After 10 min of recovery at room temperature, the oocytes were cultured in KSOM as above until used for experiments.

In vitro fertilization

Cumulus-intact oocytes were collected in 0.2 ml of HTF medium [31] and inseminated with capacitated spermatozoa (final concentration 100/μl) [32]. After 2 h incubation at 37 °C under 5% CO_2 in air, the cumulus cells were dispersed by pipetting and cultured in KSOM as above for 96 h.

SCNT and embryo transfer

The SCNT procedure was performed as described [4]. Groups of oocytes were transferred into a droplet of H-CZB containing 5 μg/ml cytochalasin B (CB) for enucleation of the second meiotic division (MII) spindle. Oocytes undergoing microsurgery were held with a holding pipette and a hole was made in the zona pellucida following the application of several piezo pulses (Prime Tech, Ibaraki, Japan) to an enucleation pipette. The MII chromosome–spindle complex was aspirated into the pipette with a minimal volume of ooplasm. After enucleation of all oocytes, they were each injected with a cumulus cell nucleus. After nuclear transfer, the reconstructed oocytes were activated using 10 mM $SrCl_2$ in KSOM with 2 mM EGTA [33] in the presence of 5 μg/ml CB for 6 h or 5 μM LatA for 10 h. In both group, 50 nM TSA treatment was continued for 10 h [11]. Activation time of 10 h is longer than usual method, but full term development of cloned embryos was not affected by longer treatment of $SrCl_2$ [20]. In some experiments, 3 nM BIX was added together with TSA. Some cloned embryos were fixed for immunostaining and other cloned embryos were cultured in KSOM at 37 °C under 5% CO_2 after three washes in

KSOM. The preimplantation development rates of cloned embryos were examined from the PN to the blastocyst stages.

Embryo transfer and examination of placentae

To produce placenta in the LatA and CB experiments, ICSI-generated and cloned embryos at the 2-cell stage were transferred into the oviducts of pseudopregnant ICR females at 0.5 days postcoitus (dpc) and placentas were collected by caesarean section at 19.5 dpc. Placental weights were measured at the time of caesarean section and the placentas were fixed with 4% paraformaldehyde (PFA) for paraffin wax embedding and histology. The placentae were sectioned for staining with hematoxylin and eosin. In the BIX treatment experiments, cloned embryos at the morula stage were transferred into the uteri of pseudopregnant ICR females at 2.5 dpc and the live offspring were collected by caesarean section at 19.5 dpc.

Live cell imaging

Chromosomal dynamics during the first, second and third mitotic division of ICSI and cloned embryos were analyzed using live cell imaging technology. Messenger RNAs encoding EGFP–α-tubulin and mRFP–H2B were prepared as described [34]. Briefly, after linearization of the template plasmid at the Xba I site, mRNA was synthesized using the T7 RiboMAX™ Large Scale RNA Production System (Promega, Madison, WI, USA). The 5′ end of each mRNA was capped using Ribo m7G Cap Analog (Promega). To circumvent the integration of template DNA into the embryo genome, reaction mixtures from in vitro transcription runs were treated with RQ-1 RNase-free DNase I (Promega). Synthesized RNAs were treated with RQ-1 RNase-free DNase I (Promega). Synthesized RNAs were treated with phenol/chloroform followed by ethanol precipitation. After dissolution in RNase-free water, mRNAs were subjected to gel filtration using a MicroSpin™ G-25 column (Amersham Biosciences, Piscataway, NJ, USA) to remove unreacted substrates and then stored at -80 °C until used. Microinjection of mRNAs into oocytes was performed as described [35]. ICSI-generated or reconstructed oocytes were transferred to droplets of H-CZB medium in the observation chamber and a few picoliters of mRNA solution were introduced into the oocyte cytoplasm using a piezo-activated micromanipulator with a glass micropipette (1–3 μm diameter). The embryos were transferred to 5 μl drops of CZB medium on a glass-bottomed dish and placed in an incubation chamber set at 37 °C on the microscope stage. A gas mixture of 5% CO_2 and 95% air was introduced into the chamber. Fifty-one images in the z-axis and two color images were captured at 15 min intervals using a live cell imaging system [34]. Device control and image analysis were performed using MetaMorph software (Molecular Devices, Sunnyvale, CA, USA).

Immunostaining

Embryos at 10 h after activation were fixed in PBS containing 4% paraformaldehyde for 30 min. The fixed oocytes were washed twice in PBS containing 1% (w/v) BSA (Nacalai Tesque, Kyoto, Japan) (PBS-BSA) for 15 min each and then stored in PBS-BSA containing 0.1% (v/v) Triton X-100 (Nacalai Tesque) overnight at 4 °C. Embryos were then incubated with the primary antibodies: rabbit polyclonal anti-acH3K9 (1:100 dilution, Upstate Biotechnology Inc., Lake Placid, NY, USA), rabbit polyclonal anti-acH3K14 (1:100 dilution; Upstate Biotechnology Inc.), rabbit polyclonal anti-H3K9me2 (1:200 dilution; Millipore, Billerica, MA, USA), rabbit monoclonal anti-H3K4me2 (1:100 dilution; Abcam Japan, Tokyo, Japan) or goat polyclonal anti-heterochromatin protein (HP) 1α (1:100; Santa Cruz Biochemicals, Santa Cruz, CA, USA) and mouse monoclonal anti-H2B (1:400 dilution; Abcam Japan) in PBS-BSA overnight at 4 °C. After the embryos had been washed twice in PBS-BSA for 15 min each, they were incubated for 1 h with dye-conjugated secondary antibodies: Alexa-Fluor 488-labeled goat anti-mouse IgG (Molecular Probes Inc., Eugene, OR) and Alexa-Fluor 546-labeled goat anti-rabbit IgG (Molecular Probes Inc.). After the embryos had been washed twice in PBS-BSA, the DNA in embryos not stained with the anti-H2B antibody was stained with 2 μg/ml of DAPI (Molecular Probes Inc.). Then, after the embryos had been washed twice in PBS-BSA, serial images were taken using fluorescence confocal microscopy (FV-1000, Olympus Corp., Tokyo, Japan). Relative levels of acH3K9, acH3K14, H3K9me2, H3K4me2 and HP1α in embryos were measured using Olympus Fluor View (Olympus). Embryos were examined in PBS at 25 °C.

Real-time RT–PCR

Complementary DNA sequences from single ICSI-generated or cloned blastocysts were synthesized using Arcturus PicoPure RNA Isolation kits (Life Technologies, Carlsbad, CA, USA). Quantitative PCR was carried out on a StepOnePlus Real-Time RT–PCR system (Applied Biosystems, Foster City, CA, USA) using Fast SYBR Green Master Mix (Applied Biosystems). The *Gapdh* gene in each embryo was used for endogenous reference. The data on gene expression levels were analyzed using StepOnePlus software (Applied Biosystems). Primer sequences were as follows: 5′-gctccaactcctctgacctg-3′ and 5′-tgtccaatgagggtacagca-3′ for *Magea2*; 5′-agcagaattcaaggcaggag-3′ and 5′-gtccatctcaaccagccaat-3′ for *Xlr5c*; and 5′-ttcaccaccatggagaaggc-3′ and 5′-ccctttggctccaccct-3′ for *Gapdh*.

Statistical analysis

The incidence of ACS, blastocyst formation rates and offspring birth rates were evaluated using Chi-squared tests. Fluorescence levels, gene expression levels, and placental weights were analyzed by ANOVA followed by Fisher's protected least significant difference test; $P < 0.05$ was assumed to be statistically significant.

Results

Abnormal chromosomal segregation (ACS) during early embryogenesis

In a previous study, we reported that abnormal F-actin localization in cloned embryos was corrected by using LatA treatment [20]. Among many roles of F-actin in the cytoplasm,